GEOPHYSICAL RESEARCH LETTERS, VOL. 28, NO. 15, PAGES 3031-3034, AUGUST 1, 2001

First seismic receiver functions on the Moon

Lev Vinnik [1]

Institute of physics of the Earth, Moscow, Russia

Hugues Chenet, Jeannine Gagnepain-Beyneix, and Philippe Lognonne

Institut de Physique du Globe de Paris, Paris, France

Abstract. We applied the S receiver function technique [*Farra and Vinnik*, 2000] to the recordings of deep moonquakes at seismograph station Apollo 12 in order to detect phases converted (Sp) and reflected beneath the station. We detected Sp phases from the base of the surficial low-velocity zone and from the mantle-crust boundary. The average P velocity in the surficial layer 1 km thick should be a few times higher than in reference model [*Toksoz et al.*, 1974]. The observed time, amplitude and waveform of Sp phase from the mantle-crust boundary are close to those predicted by the reference model but with a modified surficial layer. The S wavetrains within the first 10 s may contain waves scattered in the mantle. This scattering is stronger than in the Earth at comparable depths. The polarized component in the coda waves that we observe is another previously unknown phenomenon.

Introduction

In 1969-1972 the network of four three-component seismograph stations was deployed at the Moon by Apollo missions (see *Lognonne and Mosser* [1993] for a general review). The crustal model [*Toksoz et al.*, 1974; *Goins et al.*, 1981] (Table 1, hereafter reference model) is based mainly on observations of the first P wave arrivals from active seismic experiments at Apollo 14, 16 and 17 landing sites [*Cooper et al.*, 1974] and from artificial impacts at a minimum epicentral distance of 67 km. We describe our analysis of lunar seismic recordings with the S receiver function technique [*Farra and Vinnik*, 2000], very different from seismic techniques used previously in the lunar exploration. The method was applied to the seismograms with the longest period of 2 s.

Data and results

We look for the phases, which are related to S but arrive at the receiver as P (see examples in Figure 1). Sp phase is formed by conversion from S to P beneath the seismograph station. The other phases, like Sssp, are formed by multiple reflections. Our technique is suitable only for deep moonquakes, because their S waves are much stronger than the coda of the P waves. The SV wave of deep moonquakes is polarized practically in the radial (R) direction. The secondary phases are coupled with SV and polarized close to the vertical (Z) direction.

Deep moonquakes are very weak, but the recordings with the same source location match each other in nearly every detail for their entire duration [*Lammlein et al.*, 1974]. This similarity allows to enhance the amplitudes by stacking the records of every group [*Nakamura*, 1983]. The secondary phases, much weaker than S, can only be detected in summary recordings with extremely weak or missing coda of the direct P wave, as in example in Figure 2. At station Apollo 12 (coordinates 3.04 S, 23.42 W) we have found 13 summary recordings (Table 2) of a quality comparable to that in Figure 2. We have relocated the hypocenters in Table 2 with the aid of the velocity model by *Nakamura* [1983]. At station 14, Z component is missing for most events. Z component of station 15 is anomalously noisy. Recordings of station 16 are comparable in quality with those of station 12, but Sp phases could not be detected. We have positive results only at station 12, and these data will be presented in further detail.

We deconvolve the R and Z components of each record by the R component of the S wave. Deconvolution is performed in time domain with a proper regularization. The deconvolution filter is calculated in the time interval 10 - 20 s long. The time response of the deconvolution filter is twice shorter than this interval. In the deconvolved R component the S wave looks like a 'bump' (Figure 2). The deconvolution

Table 1. Reference (left) and preferred (right) models

Dep	V_p	V_s	ρ	V_p	V_s	ρ
0.0	0.5	0.3	2.0	2.0	1.0	2.5
0.6	0.5	0.3	2.0	2.0	1.0	2.5
1.0	0.5	0.3	2.0	3.0	1.7	2.9
1.0	4.0	2.3	3.2	3.0	1.7	2.9
1.4	4.1	2.4	3.2	4.1	2.4	3.2
4.0	4.6	2.7	3.2			
7.0	5.1	3.0	3.2			
10.0	5.4	3.1	3.2			
15.0	5.8	3.4	3.2			
20.0	6.1	3.5	3.2			
21.3	6.7	3.9	3.0			
54.5	6.7	3.9	3.0			
57.5	8.2	4.7	3.4			
65.0	8.9	5.1	3.4			

Dep is depth in km, V_p and V_s are P and S velocities in km/s, ρ is density in g/cm^3. Deeper than 1.4 km the preferred model is similar to the reference model.

[1]Also at Institut de Physique du Globe de Paris, Paris, France.

Paper number 2001GL012859.
0094-8276/01/2001GL012859$05.00

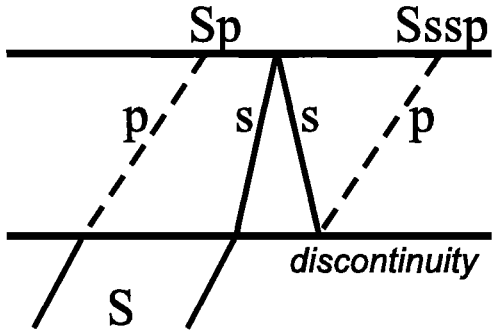

Figure 1. Raypaths of phases Sp and Sssp.

standardizes the secondary phases, as well, and they can be detected by stacking the records of many seismic events with appropriate moveout time corrections. The records were additionally filtered with a low-pass filter with a corner at 1.2 s. The whole set of the deconvolved and filtered R and Z components is shown in Figure 3.

The expected time interval between the secondary phase and S in first order approximation is a linear function of the ray parameter of the S wave. The moveout time correction for the record with a ray parameter p_1 is calculated as $a(p_1 - p_0)$, where p_0 is the average value of p for the given set of records. Parameter a for Sp phases is positive, and its value depends on the depth of the discontinuity. The stacked Z components are shown in Figure 4a. The different traces are obtained for the values of a between -0.02 and 0.02.

To invert the data in Figure 4a for a velocity model, they are compared with theoretical seismograms for plane waves propagating from the half space through the stack of plane isotropic layers. For the incoming SV wave, the spectra of the R and Z components at the free surface are related via the corresponding transfer functions $H_R(\omega)$ and $H_Z(\omega)$ as:

$$Z(\omega) = R(\omega)H_Z(\omega)/H_R(\omega) \quad (1)$$

We calculate the transfer functions for the given model with the Thomson-Haskell algorithm [*Haskell*, 1962]. The sum of the deconvolved R components (Figure 3) is used as an input. $Z(\omega)$ is obtained via Eq. (1), and the corresponding function of time is obtained by inverse Fourier transformation. We calculate the theoretical Z components for the slowness values of the actual seismograms, and then stack them like the actual seismograms.

Figure 4b shows the stack of the synthetic Z components for our preferred model (Table 1). Both theoretical and

Table 2. Deep moonquakes used in the analysis

No	*Lon*°	*Lat*°	*Dis*°	*Baz*°	Dep,km
A5	20.4	-41.0	29.1	-35.6	703
A6	42.8	55.0	83.6	46.3	853
A7	24.6	53.8	79.7	64.3	875
A8	-36.0	-36.4	35.1	-161.6	933
A9	-7.7	-16.5	8.3	124.4	995
A10	-47.6	-23.5	44.6	-179.9	933
A14	-24.7	-36.6	25.1	-150.8	933
A18	22.9	32.1	60.0	61.3	915
A20	24.2	-34.6	29.3	-21.2	969
A21	-13.0	-38.6	18.0	-124.4	969
A30	11.9	-34.9	18.8	-37.2	918
A40	-1.4	-11.8	11.7	82.2	898
A42	24.4	-54.8	41.0	-46.3	925

Dis is epicentral distance, Baz is back azimuth, positive directions for Lon and Lat are East and North.

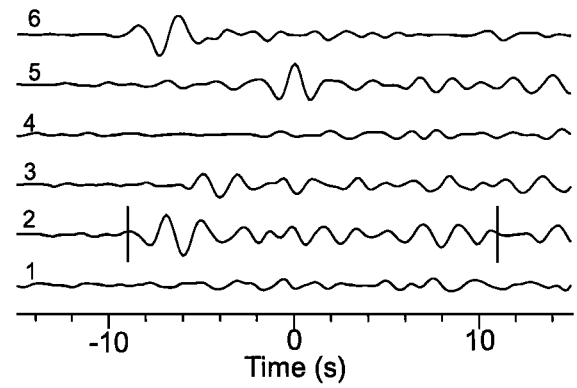

Figure 2. Traces 1-3 are Z, R and T (transverse) components of the S wave of summary event A9. Traces 4, 5 are deconvolved traces 1 and 2. The interval for deconvolution is marked by vertical bars. Trace 6 shows S wave of a typical deep earthquake; depth and epicentral distance are 573 km and 75.8°.

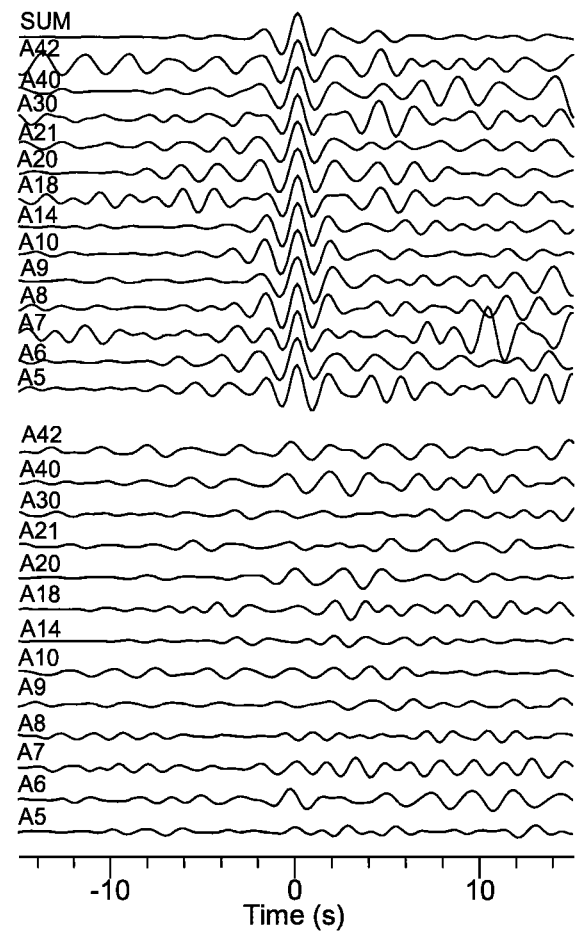

Figure 3. Deconvolved R (top) and Z (bottom) components for the events in Table 2. The trace SUM is obtained by summation of the R components.

observed stack contain an M-shaped phase (1,2), which arrives at about -8 s. In the theoretical stack this phase is focused at a positive value of a, and a similar trend is seen in the observations. This is the Sp phase from the mantle-crust transition. The other M-shaped phase (3,4) arrives at -0.4 s in both observed and synthetic seismograms. This is the Sp phase from the bottom of the surficial low-velocity layer. The Sssp phase (Figure 1) may contribute to the second pulse (4). The stack of the synthetics for the reference model (Figure 4c) looks very different from that in Figure 4a: pulses 3 and 4 in Figure 4c arrive about 1 s earlier and 2 s later, respectively, than in Figure 4a.

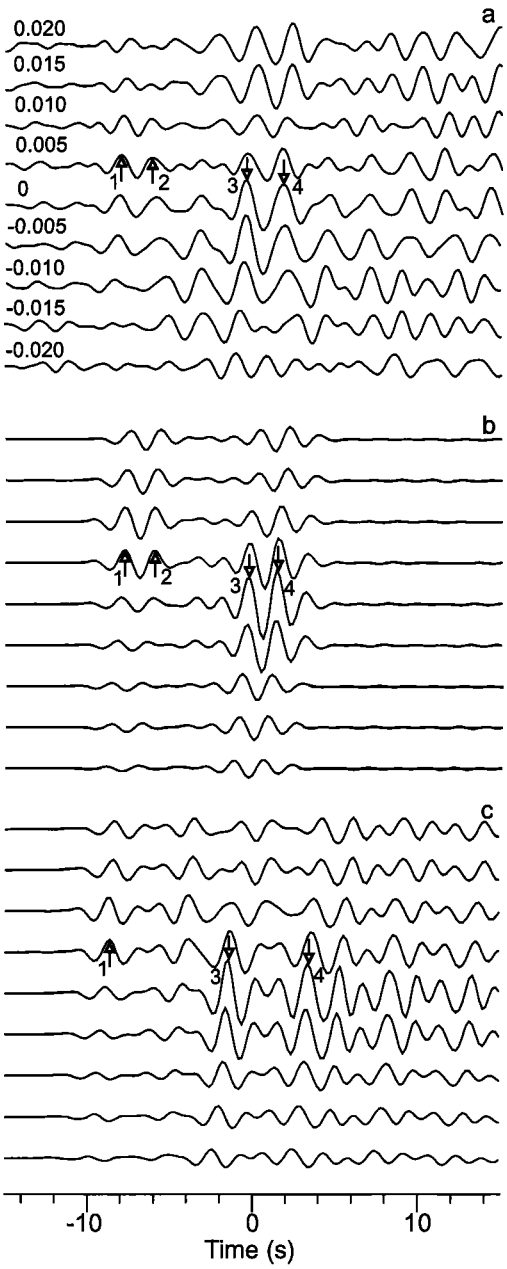

Figure 4. Stacked Z components from Figure 3, stacked synthetic Z components for our preferred model, and for reference model (a,b, and c, respectively). Moveout corrections for stacking are calculated for the values of a shown on the left in (a). The corrections depend on a and the ray parameter values of the S waves. Origin of the time scale is the same as in Figure 3. Detected signals are marked by arrows.

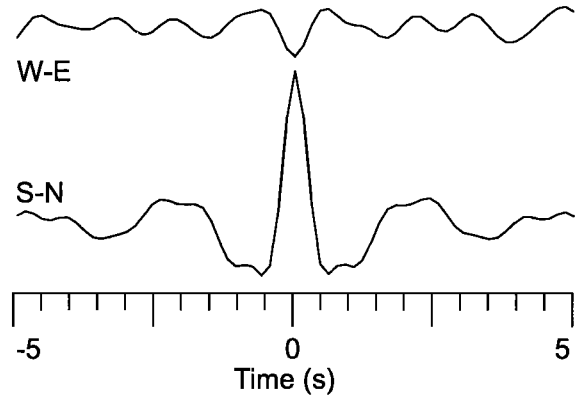

Figure 5. S-N and W-E components for source A9 deconvolved by S-N component. The interval for deconvolution is 10 minutes long.

Previous analyses emphasized chaotic structure of the codas of recordings [*Toksoz et al.*, 1974]. Our analysis reveals a correlation between the horizontal components in all recordings of deep moonquakes at station 12. As example, Figure 5 shows two horizontal components deconvolved by the S-N component. This transformation detects in the W-E component the signal with the opposite polarity and amplitude of around 20% of the S-N component. The signal in the horizontal components is polarized in the azimuth around $-60°$ irrespective of the back azimuth of the seismic source. A similar result is obtained by deconvolving the seismograms by the E-W component. No correlation is found between Z and horizontal components of station 12 or between any components of the other stations.

Discussion and conclusions

P velocity in the upper layer of the crust in our preferred model (2 km/s) is 4 times higher than in the reference model (Table 1). The optimum model, however, is not unique. The synthetics for an acceptable model must contain the Sp phase from the base of the low-velocity layer with a lead time of around 0.4 s relative to S. This time can be obtained by increasing the velocities in the layer relative to the reference model, or/and by reducing the layer thickness. Seismic data obtained at Apollo 14, 16, and 17 landing sites for the shallow crust reveal P velocity of around 0.3 km/s [*Cooper et al.*, 1974]. For this velocity, the depth of the high-velocity basement at station 12 should be about 150 m, much less than in the reference model (1 km). For any acceptable model, the average P velocity in the uppermost crustal layer with a thickness of 1 km should be a few times higher than in the reference model. The material of the low-velocity layer is interpreted as broken and fractured, and our data imply that beneath station 12 this layer is thinner or/and less fractured than can be inferred from the reference model. This might be a reason for seismic transparency of the crust beneath this station. The future Japanese LUNAR-A mission, which will deploy one station near station 12 [*Mizutani*, 1995] will take benefit from this transparency.

The time, amplitude and waveform of Sp phase from the mantle-crust boundary are very similar in Figures 4a and 4b. Thus the data lend support to the reference model with a modified surficial layer. Nevertheless, models with different

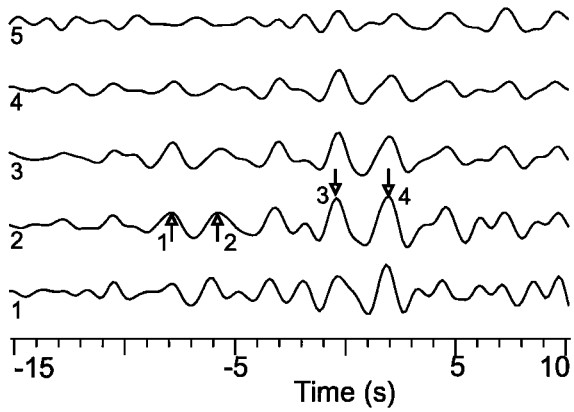

Figure 6. The same as trace $a = 0$ in Figure 4a, but for different intervals for deconvolution: 1 - 10 s, 2 - 15 s, 3 - 20 s, 4 - 30 s, 5 - 50 s.

crustal velocities and thickness may exist that fit the data equally well.

Our technique assumes that the recorded S waveforms are not distorted by random wave scattering above the discontinuity. Otherwise the corresponding Sp phases can not be standardized by deconvolution and enhanced by stacking. The effect of length of the time interval used for deconvolution is demonstrated in Figure 6. Amplitudes of the Sp phases are stable for the intervals up to 20 s long. The signals deteriorate when the interval is longer. This is a result of the increased contribution of the waves scattered in the upper crust.

Deep moonquakes demonstrate properties of shear dislocation [*Lammlein et al.*, 1974], and their magnitudes are between 0.5 and 1.3 on the Richter scale. Well known scaling relationships suggest that the duration of rupture for such events is on the order of a fraction of a second, and the duration of the emitted pulse in a frequency range around 0.5 Hz is not longer than 5 s. Continuing oscillations in the S wavetrain after the initial 5 s (Figure 2) can be attrbuted to scattering, but, as suggested by the data in Figure 6, the waves scattered in the crust arrive later. These considerations suggest that the early arrivals in the S wavetrain after 5 s can be caused by scattering in the mantle. For comparison, Figure 2 shows a typical record of deep earthquake. The waves presumably scattered in the mantle of the Moon are much stronger, although the wavepath for the deep moonquake is much shorter than for the earthquake.

Seismic coda on the Moon can be regarded as a diffusion process with isotropic distribution of directions of propagations of energy [*Toksoz et al.*, 1974]. However, the correlation between the horizontal components of motion at station 12 contradicts this. The correlation can be caused by Love waves, perhaps their higher modes which propagate at larger depths. The stable direction of propagation suggests that there is some fabric in the crust, perhaps faults with a preferred orientation.

Acknowledgments. Support of the French team is provided by PNP and CNES. L. Vinnik was partially supported by the RFBR grant 98-05-64894. The authors acknowledge help from Veronique Farra. Comments from Y. Nakamura and two anonymous referees helped to improve the paper. This is IPGP contribution 1756.

References

Cooper, M. R., R. L. Kovach, and J. S. Watkins, Lunar near-surface structure, *Rev. Geoph. Space Phys. 12,* 291-308, 1974.

Farra, V. and L. Vinnik, Upper mantle stratification by P and S receiver functions, *Geophys. J. Int. 141,* 699-712, 2000.

Goins, N. R., A. M. Dainty, and M. N. Toksoz, Lunar seismology: The internal structure of the Moon, *J. Geophys. Res., 86,* 5061-5074, 1981.

Haskell, N. A., Crustal reflection of plane P and SV waves, *J. Geophys. Res., 67,* 4751-4767, 1962.

Lammlein, D. R., G. V. Latham, J. Dorman, Y. Nakamura, and M. Ewing, Lunar seismicity, structure and tectonics, *Rev. Geoph. Space Phys. 12,* 1-21, 1974.

Lognonne, P. and B. Mosser, Planetary seismology, *Surveys in Geophysics, 14,* 239-302, 1993.

Mizutani, H., Lunar interior exploration by Japanese lunar penetrator mission, Lunar-A, *J. Phys. Earth 43,* 657-670, 1995.

Nakamura, Y., Seismic velocity structure of the lunar mantle, *J. Geophys. Res., 88,* 677-686, 1983.

Toksoz, M. N., A. M. Dainty, S. C. Solomon, and K. A. Anderson, Structure of the Moon, *Rev. Geoph. Space Phys. 12,* 539-567, 1974.

H. Chenet, J. Gagnepain-Beyneix, and P. Lognonné, Départ - ement de Géophysique Spatiale et Planétaire, FRE2315/CNRS, Institut de Physique du Globe de Paris, 4 avenue de Neptune, 94107 Saint-Maur Cedex, France.
(e-mail: lognonne@ipgp.jussieu.fr)

L. Vinnik, Institute of Physics of the Earth, B. Grouzinskaya 10, Moscow 123995, Russia.

(Received January 13, 2001; revised February 28, 2001; accepted May 7, 2001.)